



## Development of a real-time RGB-D visual feedback-assisted pulmonary rehabilitation system

Wen-Ruei Tang<sup>a</sup>, Wei Su<sup>b</sup>, Jenn-Jier James Lien<sup>b</sup>, Chao-Chun Chang<sup>a,\*</sup>,  
Yi-Ting Yen<sup>a</sup>, Yau-Lin Tseng<sup>a,\*\*</sup>

<sup>a</sup> Division of Thoracic Surgery, Department of Surgery, National Cheng Kung University Hospital, Tainan, Taiwan

<sup>b</sup> Department of Computer Science and Information Engineering, National Cheng Kung University, Tainan, Taiwan

### ARTICLE INFO

#### Keywords:

Depth camera  
Noncontact thoracoabdominal movement-tracking  
pulmonary rehabilitation  
Visual feedback

### ABSTRACT

**Background:** Following surgery, perioperative pulmonary rehabilitation (PR) is important for patients with early-stage lung cancer. However, current inpatient programs are often limited in time and space, and outpatient settings have access barriers. Therefore, we aimed to develop a background-free, zero-contact thoracoabdominal movement-tracking model that is easily set up and incorporated into a pre-existing PR program or extended to home-based rehabilitation and remote monitoring. We validated its effectiveness in providing preclinical real-time RGB-D (colour-depth camera) visual feedback.

**Methods:** Twelve healthy volunteers performed deep breathing exercises following audio instruction for three cycles, followed by audio instruction and real-time visual feedback for another three cycles. In the visual feedback system, we used a RealSense™ D415 camera to capture RGB and depth images for human pose-estimation with Google MediaPipe. Target-tracking regions were defined based on the relative position of detected joints. The processed depth information of the tracking regions was visualised on a screen as a motion bar to provide real-time visual feedback of breathing intensity. Pulmonary function was simultaneously recorded using spirometric measurements, and changes in pulmonary volume were derived from respiratory airflow signals.

**Results:** Our movement-tracking model showed a very strong correlation ( $r = 0.90 \pm 0.05$ ) between thoracic motion signals and spirometric volume, and a strong correlation ( $r = 0.73 \pm 0.22$ ) between abdominal signals and spirometric volume. Displacement of the chest wall was enhanced by RGB-D visual feedback (23 vs 20 mm,  $P = 0.034$ ), and accompanied by an increased lung volume (2.58 vs 2.30 L,  $P = 0.003$ ).

**Conclusion:** We developed an easily implemented thoracoabdominal movement-tracking model and reported the positive impact of real-time RGB-D visual feedback on self-promoted external chest wall expansion, accompanied by increased internal lung volumes. This system can be extended to home-based PR.

\* **Corresponding author.** Division of Thoracic Surgery, Department of Surgery, National Cheng Kung University Hospital 138 Sheng-Li Road, Tainan 704, Taiwan.

\*\* Corresponding author

E-mail addresses: [n048127@mail.hosp.ncku.edu.tw](mailto:n048127@mail.hosp.ncku.edu.tw) (C.-C. Chang), [tsengyl@mail.ncku.edu.tw](mailto:tsengyl@mail.ncku.edu.tw) (Y.-L. Tseng).

<https://doi.org/10.1016/j.heliyon.2023.e23704>

Received 15 November 2022; Received in revised form 10 December 2023; Accepted 11 December 2023

Available online 14 December 2023

2405-8440/© 2023 The Authors. Published by Elsevier Ltd. This is an open access article under the CC BY-NC-ND license (<http://creativecommons.org/licenses/by-nc-nd/4.0/>).

## 1. Introduction

Lung cancer is among the top 10 causes of cancer death in Taiwan and remains the leading cause of cancer death worldwide [1]. Surgery is the mainstay of treatment for early-stage non-small cell lung cancer (NSCLC). In addition to a successful surgery, perioperative pulmonary rehabilitation (PR) is important [2,3]. PR consists of endurance training, breathing exercise, and sputum clearance, which can help prepare patients for surgery, minimise postoperative pulmonary complications, and promote faster recovery. Respiratory physiology involves the respiratory muscles, such as the diaphragm and intercostal muscles, and the chest and abdominal walls. The proper coordination of these muscles and movements is necessary for efficient breathing and gas exchange. If the lungs do not fully expand postoperatively or if removal of airway secretions is inadequate, pneumonia could develop, and a patient might not functionally recover to their baseline [4]. PR has been shown to reduce postoperative pulmonary complications in studies with small sample sizes [5–8]. Furthermore, perioperative PR substantially improved exercise capacity in patients undergoing lung resection in the recent PUREAIR trial [9], and in a few systematic reviews on NSCLC [10,11]. However, current inpatient PR programs are often limited in terms of time and space [12,13]. Rehabilitation physicians and physiotherapists are not available at all times, and supervised sessions are time-consuming and personnel-demanding; hence, the rehabilitation needs of patients are not fully met.

Extending rehabilitation programs outside of a hospital setting seems to be a possible solution. However, several potential problems may arise, such as accessibility, compliance, lack of supervision, and quality control. To overcome these, various technologies have recently been incorporated into extended out-of-hospital rehabilitation programs [14–18]. Although PR outside the hospital can be assisted by video and mobile technology, the patient often has inadequate chest expansion to achieve the target intensity [19]. This problem may arise because of a lack of goal setting and score feedback [12]. The positive impact of pedometer feedback has been demonstrated in a pilot study of patients with chronic obstructive pulmonary disease (COPD) [14], as well as in a systematic review of healthy individuals [20]. Besides measuring lung function, the assessment of PR results has no other objective or quantitative indicators. While wearable acquisition devices have been utilised to quantify physiological signals [17,18,21,22], they easily cause discomfort, and none of them allows unrestrained measurement of inhalation [23]. Although several light-based models of chest wall measurement have been proposed, they are cumbersome and require sophisticated settings and marker attachments [15,24,25]. Further applications of those models in home-based rehabilitation have been hindered.

To overcome the limitations of quality assessment of video-assisted rehabilitation program, we developed a thoracoabdominal

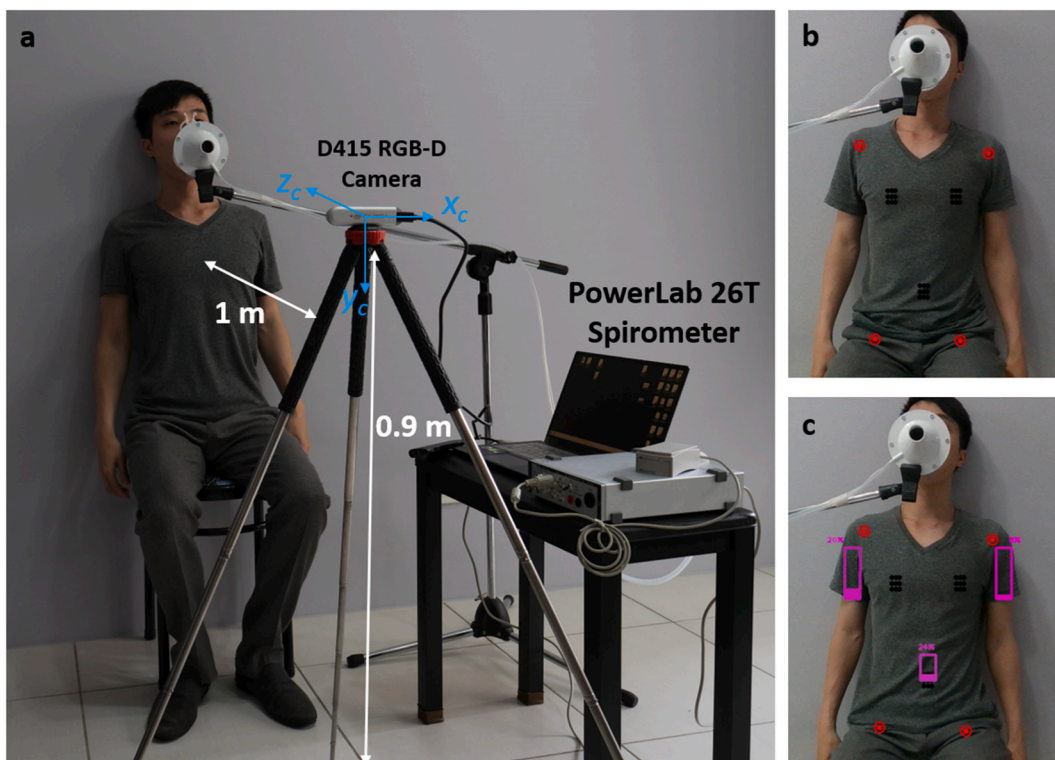


**Fig. 1. Diagram of modelling** (A) Schematic representation of real-time RGB-D visual feedback-assisted pulmonary rehabilitation system, which consists of a PowerLab 26T spirometer connected to a mouthpiece, Realsense D415 RGB-D camera, and screen (not shown). (B) Both shoulders and hip joints are detected by pose-estimation (red target circles), which is used as a reference plane to define target-tracking regions (black dots). (C) Depth information (along the z-axis of the 3D camera coordinates) of target regions are recorded over time and visualised on a screen to provide real-time visual feedback. Three motion bars (pink rectangles) represent the capacity percentages of left-chest, right-chest, and stomach regions, individually. (For interpretation of the references to colour in this figure legend, the reader is referred to the Web version of this article.)

tracking model to analyse chest wall mobilisation and showed real-time analytic results on a screen to provide visual feedback aiming at teaching breathing exercise. We hypothesised that real-time stereo visual feedback would encourage chest wall mobilisation and promote better lung movement. Our real-time RGB-D (colour-depth camera) visual feedback system that is easy to set up and which provides instant feedback to patients about the extent of their chest mobilisation. This system could be further extended to home-based PR and remote monitoring. The present study's purpose was to first describe the development of this easily set up background-free, zero-contact thoracoabdominal movement-tracking model, and, secondly, to validate its effectiveness in providing real-time RGB-D visual feedback preclinically. The outcome measures were chest wall expansion and changes in lung volume.

## 2. Methods

### 2.1. Equipment setting

As shown in Fig. 1A, volunteers were asked to sit straight with their backs against the back of an armless chair with both arms down by their sides, while breathing through a mouthpiece. A PowerLab® 26T spirometer (ADInstruments, Sydney, Australia) was used to measure flow changes through the mouthpiece, and a nose clip was applied to prevent air leakage. A Realsense™ D415 RGB-D camera (Intel Corp., Santa Clara, CA, USA) was placed 1 m in front of the volunteer, at a height of 0.9 m, such that both shoulders and hip joints of the participant were within the camera's field of view. The distance of approximately 1 m was chosen based on the ease of clinical bedside use and the measurement accuracy of the D415 [26]. Feedback of the analysis of chest wall motion was displayed on a screen 1.5 m in front of the volunteer.

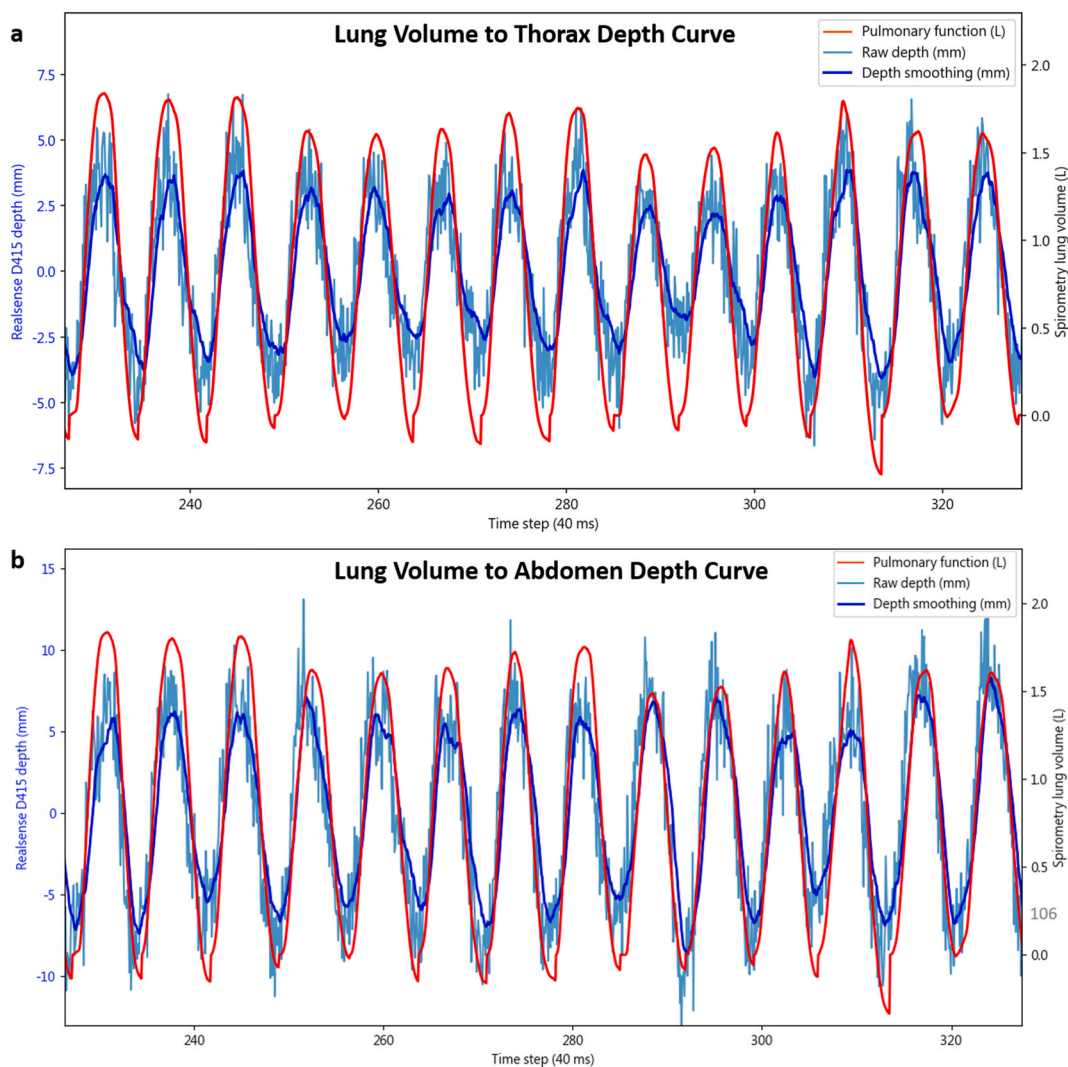


**Fig. 2.** Spirometric volume to thoracoabdominal depth information of one participant over time (A) Lung volume to thorax depth curve (B) Lung volume to abdomen depth curve. The spirometric lung volume had strong synchronisation with thoracoabdominal motion signals.

## 2.2. Data acquisition and preprocessing

In the present study, both RGB and depth images were captured using a Realsense™ D415 RGB-D camera. The RGB images were then used as inputs for human pose-estimation with Google's MediaPipe (version: 0.8.7.1) [27]. Google MediaPipe is an open-source, cross-platform framework for building multimodal machine learning pipelines, including audio, video, and sensor data processing. It offers pre-built machine learning models and functions for tasks such as object detection, face detection, hand tracking, and pose estimation. As shown in Fig. 1B, both shoulders and hip joints of one person were detected and were defined as the four corners of the reference thoracoabdominal region. The shoulder width was calculated as the distance between the shoulders. Upper body length was calculated as the distance between the shoulder and hip joints. Target-tracking regions (right chest, left chest, and abdomen) were then defined according to the relative position of the detected reference plane. The centre of the tracking region of the right chest was defined as the quarter of the shoulder width and the upper third quarter of the upper body length. The centre of the tracking region of the left chest was defined as the quarter of the shoulder width and the upper third quarter of the upper body length. The centre of the abdominal tracking region was defined as the middle of the body and the lower third quarter of the upper body. Therefore, the target-tracking regions were adjusted automatically according to different body sizes. The entire model was implemented in Python 3.8 on Windows 10 with an Intel® Core™ i7-1065G7 CPU. The source code for our program is provided in the supplementary materials.

For each healthy volunteer, we simultaneously recorded RGB-D depth information of the target-tracking regions at 25 Hz and spirometric pulmonary function at a sampling rate of 1000 Hz. The depth-recording region (target-tracking regions) contained the right and left chest and the upper abdomen. A change in pulmonary volume was derived from the integration of the respiratory airflow signal over time. As shown in Fig. 2, the raw depth information was subjected to high-frequency noise; hence, a 16-point moving-average filter was applied (corresponding to a 360-ms delay). The smoothed curve was then normalised by subtracting the mean of the sliding window. The sliding window had 127 samples before the current time (a total of 128 samples, approximately 5 s, corresponding to one respiratory cycle of 12 breaths per minute (bpm)). Finally, the normalised curve was visualised on a screen as a bar value to provide real-time visual feedback of breathing intensity (Fig. 1C). The bar moved upward during inhalation and downward during exhalation. The bar values were linearly interpolated from the maximum and minimum depth distances of the previous respiratory cycle to 0 % and 100 %, respectively. The inhalation time, exhalation time, and ratio of exhalation-to-inhalation (E/I) were determined. A demonstration video is provided in the Supplementary Material (Video 1).

## 2.3. Study design

This study was approved by the institutional review board of the National Cheng Kung University Hospital (IRB No. B-ER-111-102). Participants were included if they were aged over 20 years, literate, willing, able to provide written consent, spoke Chinese without

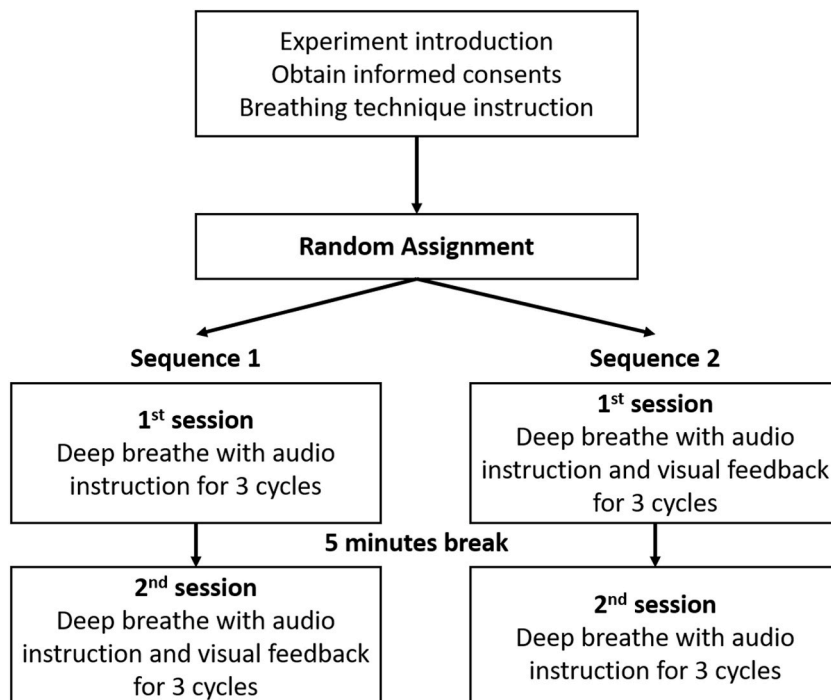


Fig. 3. Flow diagram of study design.



communication barriers, and had no known pulmonary or cardiac disease. Exclusion criteria were the inability to perform mouth breathing, pregnancy, severe kyphosis, and the inability to understand instructions in Chinese. Informed consent was obtained from all participants.

To simulate bedside rehabilitation, there were no clothing restrictions and participants wore casual clothing. As shown in Fig. 3, the experiment consisted of two sessions. Before recording, participants were instructed on how to take a deep breath by watching a PR video. The PR video was one routinely used in clinical practice at our hospital's thoracic surgery ward and is provided in the Supplementary Material (Video 2). Before starting the measurement, the spirometer was calibrated using a 3-L syringe. Participants were randomly assigned to one of two exercise sequences according to a computer-generated list. The two exercises were randomised in a cross-over design to prevent potential learning effects. While recording RGB-D depth information and spirometric volume simultaneously, one group of healthy volunteers were asked to breathe regularly for 30 s and then perform deep breathing exercises following audio instruction (AI) for three cycles, followed by both AI and visual feedback (AI-VF) for another three cycles (sequence 1). Participants in the other group first completed the AI plus AI-VF routine before performing the exercise with only AI (sequence 2). Between each session, there was a 5-min break. AI included inhaling through a mouthpiece with maximal effort as deeply as possible, and then exhaling slowly and completely.

#### 2.4. Statistical analysis

The Kolmogorov–Smirnov test was used to analyse the data distribution. Non-normally distributed numeric variables are presented as median and interquartile range (IQR), and were analysed using the Wilcoxon signed-rank test. Normally distributed continuous variables are presented as mean  $\pm$  standard deviation (SD). Categorical variables are presented as counts (percentages). Pearson's correlation coefficient was used to determine the relationship between the RGB-D depth information and spirometer-derived volume. A value of  $P < 0.05$  was considered to indicate significance. Statistical analyses were performed using SPSS version 20.0 Windows (IBM SPSS Corp., Armonk, NY, USA).

### 3. Results

As demonstrated in Fig. 2, our proposed tracking model showed a strong synchronisation between thoracoabdominal motion signals and spirometric pulmonary volume. Pearson correlation coefficients showed a very strong correlation ( $r = 0.90 \pm 0.05$ ) between thoracic motion signals and spirometric volume and a strong correlation ( $r = 0.73 \pm 0.22$ ) between abdominal signals and spirometric volume (Fig. 4). When respiratory rate estimated by our model was compared to that of a standard spirometer, a mean (range) bias of 0.0 (−0.5 to 0.5) bpm was noted. The mean  $\pm$  SD of respiratory rate in the 12 participants was  $10.1 \pm 3.2$  bpm.

Twelve healthy volunteers participated in this study. The demographic data are summarised in Table 1. The median (IQR) age was 29 (28–29) years, and half of the participants were male. Body size was larger in men than in women (height: 171 vs 159 cm,  $P = 0.009$ ; weight: 70 vs 54 kg,  $P = 0.015$ ). As shown in Table 2, the chest wall displacement was enhanced with real-time RGB-D visual feedback (23 vs 20 mm,  $P = 0.034$ ), and was accompanied by increased lung volume (2.58 vs 2.30 L,  $P = 0.003$ ). Nevertheless, there was no significant change in the upper abdomen displacement (9.2 vs 8.7 mm,  $P = 0.929$ ). The augmentation effect of the added visual feedback during the deep breathing exercises was independent of the intervention sequence (Table 3).

A scatter plot showed a distinct difference in volume to chest motion distance between the male and female participants (Fig. 5). However, in terms of the gap between AI-VF and AI, there was no significant difference in the volume change and motion distance increase between the sexes (Table 4).

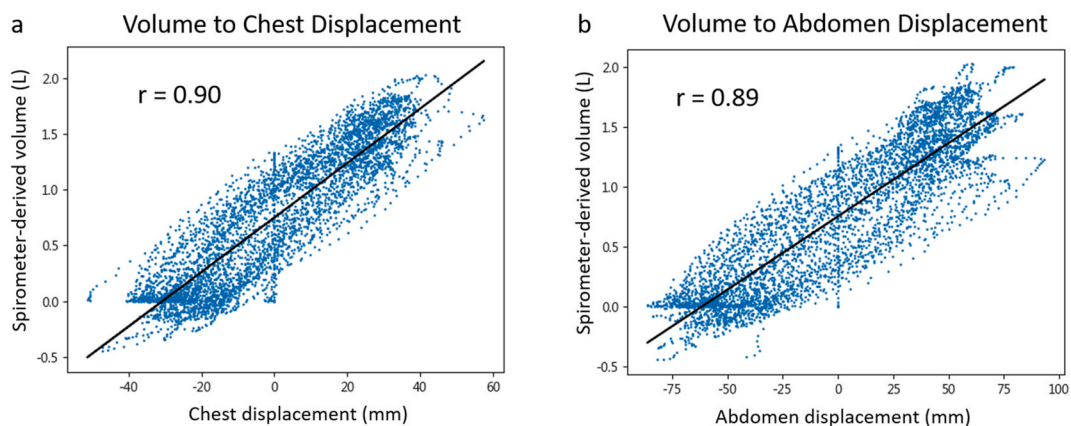


**Fig. 4.** Correlation of volume and depth information in one participant (A) Correlation between spirometer-derived volume and chest displacement in one participant. The Pearson correlation coefficient was 0.90. (B) Correlation between spirometer-derived volume and abdomen displacement in one participant. The Pearson correlation coefficient was 0.89.

**Table 1**  
Baseline characteristics of 12 healthy participants.

	Total N = 12	Male N = 6	Female N = 6	P
Age, y	29 (28–29)	29 (28–29)	29 (28–31)	0.937
Height, cm	167 (159–170)	171 (168–176)	159 (155–167)	0.009
Weight, kg	60 (51–69)	70 (63–86)	54 (45–60)	0.015
BMI, kg/m <sup>2</sup>	22.0 (19.5–24.4)	23.9 (21.2–29.6)	20.6 (18.7–22.1)	0.093
Current smokers	0 (0.0)	0 (0.0)	0 (0.0)	NA

BMI, body mass index.

**Table 2**  
Outcomes in audio instruction with real-time visual feedback compared with audio instruction alone.

	Audio instruction (AI)	AI with visual feedback (AI-VF)	P
Spirometric volume, L	2.30 (1.92–3.42)	2.58 (2.00–3.85)	0.003
Chest motion, mm	20 (13–27)	23 (15–28)	0.034
Abdomen motion, mm	9 (5–25)	9 (7–26)	0.929

**Table 3**  
Comparison between sequence 1 and sequence 2.

	Group of sequence 1 N = 6	Group of sequence 2 N = 6	p
Age, y	29 (28–31)	29 (28–29)	0.485
Sex (male)	3 (50.0)	3 (50.0)	>0.999
Height, cm	169 (159–172)	164 (155–173)	0.485
Weight, kg	59 (50–86)	64 (48–69)	0.937
BMI, kg/m <sup>2</sup>	22.0 (17.9–28.8)	22.0 (20.3–23.9)	>0.999
AI			
Volume, L	2.30 (2.06–3.07)	2.60 (1.61–3.47)	0.699
Thorax, mm	20 (16–28)	19 (8–28)	0.589
Abdomen, mm	24 (13–31)	5 (5–8)	0.004
AI-VF			
Volume, L	2.58 (2.27–3.75)	2.83 (1.79–3.94)	0.699
Thorax, mm	23 (21–27)	20 (9–30)	0.818
Abdomen, mm	24 (16–30)	8 (7–9)	0.082
Difference (AI-VF – AI)			
Volume, L	0.20 (0.11–0.56)	0.25 (0.21–0.47)	0.589
Thorax, mm	4 (0–5)	1 (0–2)	0.662
Abdomen, mm	–1 (–12–6)	1 (0–5)	0.065

AI, audio instruction; AI-VF, AI with visual feedback; BMI, body mass index.

#### 4. Discussion

Perioperative PR is critical after thoracic surgery. Despite this, current PR programs face many obstacles, from inpatient care to outpatient care to home-based services [12,13,28–32]. Our proposed thoracoabdominal wall-tracking model addresses several challenges encountered in previous studies and can be integrated into pre-existing rehabilitation programs ranging from hospital-to-home-based courses. By applying deep learning-based pose-detection methods, we eliminated the need for attached markers, dazzling light projectors, and the wearable devices used in other studies [15,22,33]. Without the requirement for attached sensors, the possibility of a sensor displacement [18] was avoided. Moreover, by subtracting the mean of the sliding window, the participant was assigned the datum origin. Following this algorithm, the distance between the participant and camera was not restricted, and the baseline was automatically recalibrated once the participant moved. Hence, there was no need to define the origin of the coordinates in advance. Furthermore, the right and left hemithorax and abdomen were defined separately, and feedback was provided individually, which is particularly important in unilateral thoracic surgery. It is vital that patients practice focused segmental breathing on the operated side rather than compensatory breathing on the non-operated side. Assistance in learning diaphragmatic breathing via abdominal feedback was also helpful. It should be noted that there was always a positive correlation in the chest wall signals; however, a negative correlation with the abdominal signals could occur because of paradoxical movements during forced breathing. These correlations could be used to analyse abnormal breathing patterns in future studies. In addition, our proposed model can be applied not only to group rehabilitation programs via multi-person pose-estimation, but also to telerehabilitation through cloud computing technology and wireless connectivity.

Proper rehabilitation techniques are crucial for enhancing efficient recovery. In contrast to orthopaedic systems that emphasise range of motion of a joint, which can be seen easily by the patient, the work of respiratory muscles is difficult to feel. Unlike dyspnoeic

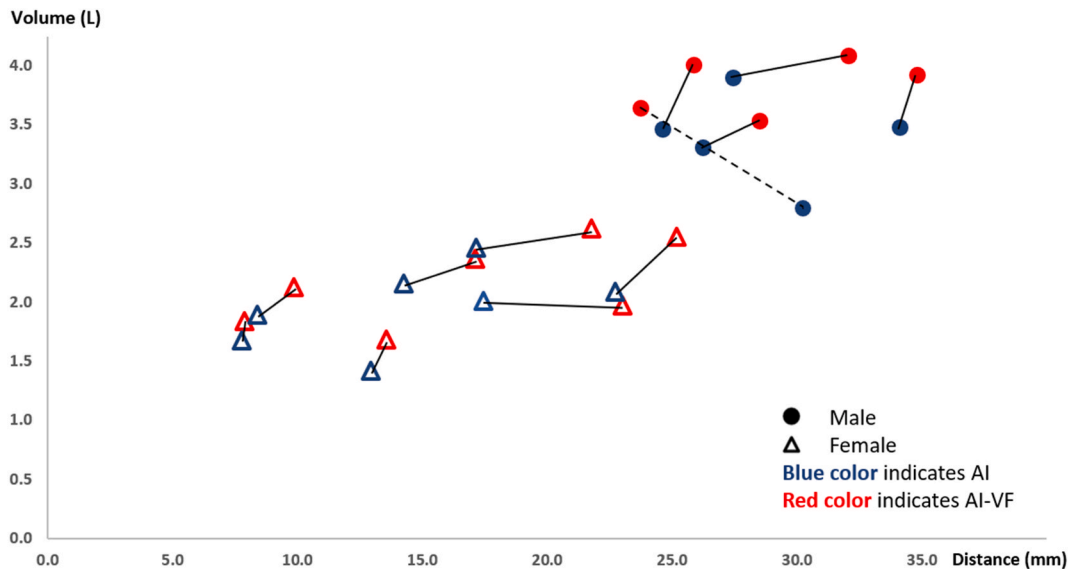


Fig. 5. Scatterplot of volume to chest motion distance during AI and AI-VF pairs.

Table 4

Comparison of outcomes of men and women.

	Men N = 6	Women N = 6	P
AI			
Volume, L	3.38 (2.61–3.87)	1.95 (1.64–2.23)	0.009
Thorax, mm	27 (24–31)	14 (8–17)	0.002
Abdomen, mm	16 (3–31)	8 (5–17)	0.818
AI-VF			
Volume, L	3.78 (3.29–4.03)	2.04 (1.79–2.43)	0.004
Thorax, mm	27 (25–33)	15 (9–22)	0.002
Abdomen, mm	15 (6–28)	8 (6–22)	0.485
Difference (AI-VF – AI)			
Volume, L	0.35 (0.15–0.62)	0.19 (0.09–0.24)	0.240
Thorax, mm	2 (-1–3)	2 (0–5)	0.699
Abdomen, mm	0 (-8–5)	2 (-3–6)	0.699

AI, audio instruction; AI-VF, AI with visual feedback.

patients with COPD who focus on exercise training because of chronic skeletal muscle dysfunction, patients with NSCLC face temporary chest wall deconditioning with severely impaired pulmonary function following intensive treatment of their diseases [2]. Through our algorithm, participants observed how the chest wall moved with their own eyes while taking a deep breath. Instead of struggling with vague chest movements, participants watched their breathing directly. In our study, real-time visual feedback effectively supported and guided target chest wall movement (23 vs 20 mm,  $P = 0.034$ ); therefore, participants’ breathing deepened (2.58 vs 2.30 L,  $P = 0.003$ ). Additionally, these benefits were independent of sex and body size. Nevertheless, the clinical implications of these slight differences should be interpreted with caution. There was no difference in abdominal movement distance ( $P = 0.929$ ), which could be attributed to clothing wrinkles in a sitting posture. This external factor might explain, at least in part, the slightly lower correlation coefficient between abdominal signals and spirometer measurements ( $r = 0.73 \pm 0.22$ ). In addition to clothing wrinkles, anteroposterior body postural sway also influenced the measurement accuracy. As shown in Fig. 5, one participant (dashed line) showed an increased lung volume accompanied by a decrease in chest wall expansion. This was caused by slight leaning forward on expiration and leaning backward on inspiration. This body displacement offsets the depth information for the chest wall movements. Recent studies have used electrical impedance tomography (EIT) to guide PR and monitor ventilation at bedside [33]. As its name suggests, EIT monitors lung ventilation by measuring electrical conductivity. Therefore, an electrode belt is used, which greatly increases discomfort and risks skin irritation during rehabilitation. Additionally, EIT is criticized for its sensitivity to electrode placement and interpretation complexity.

Apart from the small sample size, our study had several limitations. First, all participants were healthy and literate, without physical suffering, which is markedly different from patients who have undergone surgery. In addition, as we enrolled 12 healthy volunteers, no long-term clinical outcomes were observed. Hence, the clinical significance of increased chest wall motion and lung volume was not determined in the present study and should be interpreted with caution. Second, the study was not blinded. However,

since the outcome measures were objective, we believe that the results were credible. Third, the anteroposterior body postural sway greatly influenced the measurement accuracy of chest wall motion. Therefore, we asked participants to sit straight with their backs against the back of the chair to minimise movement noise, given the relatively small displacement that occurs during breathing. Nonetheless, the lung volume measurement was not affected, and the effectiveness of RGB-D visual feedback was supported. Fourth, patient-centred outcomes and user experiences were not evaluated. Fifth, our model only indirectly correlates chest wall motion to lung ventilation without providing insight into underlying physiological processes like EIT and spirometry.

Larger trials with clinically relevant outcomes are required in the future to corroborate our findings. Similarly, patient-reported outcomes regarding adherence, convenience of use, and quality of life should be assessed. It is noteworthy that the modification of static or dynamic lung function might not occur in patients with chronic airway obstruction [34]. Therefore, proper selection of the study population is crucial.

## 5. Conclusion

We have developed an easily implemented thoracoabdominal movement-tracking model and reported the positive impact of real-time RGB-D visual feedback in self-promoted external chest wall expansion, accompanied by increased internal lung volume mobilisation. This system can extend the availability of PR to patients at home or in outpatient-based programs. Nevertheless, an adequately powered randomised controlled trial with clinically relevant outcomes is warranted and is currently underway at our institution.

### Ethics approval and consent to participate

This study was approved by the Institutional Review Board (IRB) of National Cheng Kung University Hospital (B-ER-111-102), and performed in accordance with the Declaration of Helsinki.

### Financial disclosures

The study was supported by Ministry of Science and Technology (MOST-111-2314-B-006-106), National Cheng Kung University Hospital of Taiwan (NCKUH-11103026), and Department of Surgery Research Gap Year Program, National Cheng Kung University Hospital of Taiwan (NCKUH B227).

### Other contributions

We thank the Department of Physiology, College of Medicine, National Cheng Kung University for the use of their PowerLab 26T spirometer to facilitate our research; the Department of Computer Science and Information Engineering, National Cheng Kung University for unwavering support in the use of artificial intelligence techniques; and the Institute of Allied Health Sciences, College of Medicine, National Cheng Kung University for advice on rehabilitation guidance and provision of the rehabilitation video.

### Data availability statement

Data included in article/supp. material/referenced in article.

### CRediT authorship contribution statement

**Wen-Ruei Tang:** Conceptualization, Data curation, Formal analysis, Investigation, Methodology, Project administration, Validation, Visualization, Writing – original draft. **Wei Su:** Methodology, Software, Visualization. **Jenn-Jier James Lien:** Conceptualization, Methodology, Software, Supervision. **Chao-Chun Chang:** Conceptualization, Investigation, Methodology, Project administration, Resources, Supervision, Writing – review & editing. **Yi-Ting Yen:** Resources. **Yau-Lin Tseng:** Funding acquisition, Resources.

### Declaration of competing interest

The authors declare that they have no known competing financial interests or personal relationships that could have appeared to influence the work reported in this paper.

### Appendix A. Supplementary data

Supplementary data to this article can be found online at <https://doi.org/10.1016/j.heliyon.2023.e23704>.



## References

- [1] H. Sung, J. Ferlay, R.L. Siegel, et al., Global cancer statistics 2020: GLOBOCAN estimates of incidence and mortality worldwide for 36 cancers in 185 countries, *CA Cancer J Clin* 71 (2021) 209–249, <https://doi.org/10.3322/caac.21660>.
- [2] M.A. Spruit, P.P. Janssen, S.C. Willemsen, et al., Exercise capacity before and after an 8-week multidisciplinary inpatient rehabilitation program in lung cancer patients: a pilot study, *Lung Cancer* 52 (2006) 257–260, <https://doi.org/10.1016/j.lungcan.2006.01.003>.
- [3] P.M. Kenny, M.T. King, R.C. Viney, et al., Quality of life and survival in the 2 years after surgery for non small-cell lung cancer, *J. Clin. Oncol.* 26 (2008) 233–241, <https://doi.org/10.1200/JCO.2006.07.7230>.
- [4] P. Agostini, H. Cieslik, S. Rathinam, et al., Postoperative pulmonary complications following thoracic surgery: are there any modifiable risk factors? *Thorax* 65 (2010) 815–818, <https://doi.org/10.1136/thx.2009.123083>.
- [5] V. Cavalheri, C. Granger, Preoperative exercise training for patients with non-small cell lung cancer, *Cochrane Database Syst. Rev.* 6 (2017) CD012020, <https://doi.org/10.1002/14651858.CD012020.pub2>.
- [6] H. Saito, K. Hatakeyama, H. Konno, et al., Impact of pulmonary rehabilitation on postoperative complications in patients with lung cancer and chronic obstructive pulmonary disease, *Thorax* 68 (2013) 451–460, <https://doi.org/10.1111/1759-7714.12466>.
- [7] G. Chesterfield-Thomas, I. Goldsmith, Impact of preoperative pulmonary rehabilitation on the Thoracoscore of patients undergoing lung resection, *Interact. Cardiovasc. Thorac. Surg.* 23 (2016) 729–732, <https://doi.org/10.1093/icvts/ivw238>.
- [8] A. Bradley, A. Marshall, L. Stonehewer, et al., Pulmonary rehabilitation programme for patients undergoing curative lung cancer surgery, *Eur. J. Cardio. Thorac. Surg.* 44 (2013) e266–e271, <https://doi.org/10.1093/ejcts/ezt381>.
- [9] S. Tenconi, C. Mainini, C. Rapicetta, et al., Rehabilitation for lung cancer patients undergoing surgery: results of the PUREAIR randomized trial, *Eur. J. Phys. Rehabil. Med.* 57 (2021) 1002–1011, <https://doi.org/10.23736/S1973-9087.21.06789-7>.
- [10] I.D. Rosero, R. Ramírez-Vélez, A. Lucia, et al., Systematic review and meta-analysis of randomized, controlled trials on preoperative physical exercise interventions in patients with non-small-cell lung cancer, *Cancers* 11 (2019), <https://doi.org/10.3390/cancers11070944> (Basel).
- [11] C.L. Granger, C.F. McDonald, S. Berney, et al., Exercise intervention to improve exercise capacity and health related quality of life for patients with non-small cell lung cancer: a systematic review, *Lung Cancer* 72 (2011) 139–153, <https://doi.org/10.1016/j.lungcan.2011.01.006>.
- [12] M.A. Spruit, S.J. Singh, C. Garvey, et al., An official American Thoracic Society/European Respiratory Society statement: key concepts and advances in pulmonary rehabilitation, *Am. J. Respir. Crit. Care Med.* 188 (2013) e13–e64, <https://doi.org/10.1164/rccm.201309-1634ST>.
- [13] A. Cesario, L. Ferri, D. Galetta, et al., Postoperative respiratory rehabilitation after lung resection for non-small cell lung cancer, *Lung Cancer* 57 (2007) 175–180, <https://doi.org/10.1016/j.lungcan.2007.02.017>.
- [14] B.M. de Blok, M.H. de Greef, N.H. ten Hacken, et al., The effects of a lifestyle physical activity counseling program with feedback of a pedometer during pulmonary rehabilitation in patients with COPD: a pilot study, *Patient Educ. Couns.* 61 (2006) 48–55, <https://doi.org/10.1016/j.pec.2005.02.005>.
- [15] E.G. Collins, W.E. Langbein, L. Fehr, et al., Can ventilation-feedback training augment exercise tolerance in patients with chronic obstructive pulmonary disease? *Am. J. Respir. Crit. Care Med.* 177 (2008) 844–852, <https://doi.org/10.1164/rccm.200703-477OC>.
- [16] L. Pomidori, F. Campigotto, T.M. Amaty, et al., Efficacy and tolerability of yoga breathing in patients with chronic obstructive pulmonary disease: a pilot study, *J. Cardiopulm Rehabil Prev* 29 (2009) 133–137, <https://doi.org/10.1097/HCR.0b013e31819a0227>.
- [17] A. Angelucci, D. Kuller, A. Aliverti, A home telemedicine system for continuous respiratory monitoring, *IEEE J Biomed Health Inform* 25 (2021) 1247–1256, <https://doi.org/10.1109/JBHI.2020.3012621>.
- [18] G. Brüllmann, K. Fritsch, R. Thurnheer, et al., Respiratory monitoring by inductive plethysmography in unrestrained subjects using position sensor-adjusted calibration, *Respiration* 79 (2010) 112–120, <https://doi.org/10.1159/000212117>.
- [19] C. McCabe, M. McCann, A.M. Brady, Computer and mobile technology interventions for self-management in chronic obstructive pulmonary disease, *Cochrane Database Syst. Rev.* 5 (2017) CD011425, <https://doi.org/10.1002/14651858.CD011425.pub2>.
- [20] D.M. Bravata, C. Smith-Spangler, V. Sundaram, et al., Using pedometers to increase physical activity and improve health: a systematic review, *JAMA* 298 (2007) 2296–2304, <https://doi.org/10.1001/jama.298.19.2296>.
- [21] T. Allsop, K. Carroll, G. Lloyd, et al., Application of long-period-grating sensors to respiratory plethysmography, *J. Biomed. Opt.* 12 (2007) 064003, <https://doi.org/10.1117/1.2821198>.
- [22] D. Manné, F. de Jongh, H. van Helvoort, The accuracy of tidal volume measured with a smart shirt during tasks of daily living in healthy subjects: cross-sectional study, *JMIR Form Res* 5 (2021) e30916, <https://doi.org/10.2196/30916>.
- [23] S. Jayasekera, E. Hensel, R. Robinson, Feasibility assessment of wearable respiratory monitors for ambulatory inhalation topography, *Int J Environ Res Public Health* 18 (2021), <https://doi.org/10.3390/ijerph18062990>.
- [24] R.E. Redlinger Jr., A. Wootton, R.E. Kelly, et al., Optoelectronic plethysmography demonstrates abrogation of regional chest wall motion dysfunction in patients with pectus excavatum after Nuss repair, *J. Pediatr. Surg.* 47 (2012) 160–164, <https://doi.org/10.1016/j.jpedsurg.2011.10.038>.
- [25] G. Elshafie, P. Kumar, S. Motamedi-Fakhr, et al., Measuring changes in chest wall motion after lung resection using structured light plethysmography: a feasibility study, *Interact. Cardiovasc. Thorac. Surg.* 23 (2016) 544–547, <https://doi.org/10.1093/icvts/ivw185>.
- [26] F. Lourenço, H. Araujo, Intel RealSense SR305, D415 and L515: Experimental evaluation and Comparison of depth estimation, Paper presented at: Proceedings of the 16th International Conference on Computer Vision Theory and Applications (2021), <https://doi.org/10.5220/0010254203620369>.
- [27] C. Lugaresi, J. Tang, H. Nash, et al., MediaPipe: a framework for building perception pipelines, arXiv 1906.08172 (2019). <https://ui.adsabs.harvard.edu/abs/2019arXiv190608172L>. (Accessed 1 June 2019).
- [28] F. Maltais, J. Bourbeau, S. Shapiro, et al., Effects of home-based pulmonary rehabilitation in patients with chronic obstructive pulmonary disease: a randomized trial, *Ann. Intern. Med.* 149 (2008) 869–878, <https://doi.org/10.7326/0003-4819-149-12-200812160-00006>.
- [29] J.C. Mendes de Oliveira, F.S. Studart Leitão Filho, L.M. Malosa Sampaio, et al., Outpatient vs. home-based pulmonary rehabilitation in COPD: a randomized controlled trial, *Multidiscip Respir Med* 5 (2010) 401–408, <https://doi.org/10.1186/2049-6958-5-6-401>.
- [30] M. Rispoli, R. Salvi, A. Cennamo, et al., Effectiveness of home-based preoperative pulmonary rehabilitation in COPD patients undergoing lung cancer resection, *Tumori* (2020) 300891619900808, <https://doi.org/10.1177/0300891619900808>.
- [31] A. Sbrollini, M. Morettini, E. Maranesi, et al., Sport Database: cardiorespiratory data acquired through wearable sensors while practicing sports, *Data Brief* 27 (2019) 104793, <https://doi.org/10.1016/j.dib.2019.104793>.
- [32] A. Caroppo, A. Leone, P. Siciliano, et al., Cognitive home rehabilitation in Alzheimer's disease patients by a virtual personal trainer, *Ambient Assist Living* 147–55 (2014), [https://doi.org/10.1007/978-3-319-01119-6\\_15](https://doi.org/10.1007/978-3-319-01119-6_15).
- [33] Q. Li, Y. Li, G. Niu, et al., Chest physiotherapy guided by electrical impedance tomography in high-dependency unit patients with pulmonary diseases: an introduction of methodology and feasibility, *Crit. Care* 27 (2023) 24, <https://doi.org/10.1186/s13054-023-04308-w>.
- [34] J.S. Alpert, H. Bass, M.M. Szucs, et al., Effects of physical training on hemodynamics and pulmonary function at rest and during exercise in patients with chronic obstructive pulmonary disease, *Chest* 66 (1974) 647–651, [https://doi.org/10.1016/S0012-3692\(15\)38490-7](https://doi.org/10.1016/S0012-3692(15)38490-7).